

## **Dynamic characteristics of the offshore floating platform with a mooring cable under a linear combination of wind and wave**

\*Young-Tae Lee<sup>1)</sup>, Dan Gu<sup>2)</sup> and Hee-Chang Lim<sup>3)</sup>

<sup>1), 2), 3)</sup> *School of Mechanical Engineering, Pusan National University, Busan, 609-735, Korea*

<sup>3)</sup> *hclim@pusan.ac.kr*

### **ABSTRACT**

In order to make an initial design of Spar Buoy Platform (SBP), a numerical study has been systematically performed. SBP is one of the well-known offshore floating platforms linked with the mooring cable. The primary components of SBP consist of a rotating blade, a rigid floating body, anchors and flexible elements such as mooring cables. From an engineering point of view, the rotating blade is not included in this study, but the platform and mooring cables are simply considered to observe the dynamic responses arising from the upstream wind and wave load. When the platform moves under the external loads, it is easily conjectured that the power performance would be changed and unstable. The design of the offshore floating body basically needs to understand the precise modeling of oncoming wind and wave load and the dynamic response based on the hydrostatic, hydrodynamic and gravitational forces. In this study, hydrostatic and hydrodynamic loads are formulated by a combination of the Morison formula and the pressure integration method. Based on the water depth and the wave period/height, the linear airy wave theory and non-linear Stokes wave theory can be selectively applied. The wind load is one of important parameters to design the wind blade and the floating body. It is assumed that the wind profile would be a shear layer so that as a simple case a well-known shape of a power law profile is applied. In this study, both wind and wave loads acting on the floating body are mathematically formulated, which is based on the field data. Then the dynamic response is numerically analyzed with changing the shape and the number of mooring cables under a straight tension.

### **1. INTRODUCTION**

Energy, required for maintaining modern life, has become a critical resource often

---

<sup>1)</sup> Graduate Student

<sup>2)</sup> Graduate Student

<sup>3)</sup> Professor

prematurely assumed to be available for future prosperity. Oil has reached a record-high \$112 a barrel, which is the highest level since 2008. This exigency, coupled with global warming concerns, has led to substantial research in creating inexpensive energy generation through renewable energy sources Well(2007). Wind energy is one of the most promising of these sources. In particular, converting wind energy to electricity is a concept that has gained attention because of its technological maturity, good infrastructure, and relative cost competitiveness Joselin(1998). The harvesting of wind energy is currently the fastest growing energy source. Its annual growth rate of approximately 20% indicates that renewable energy is attractive since it offers environmental and economic advantages Ezio(1998).

Although the wind turbine can operate under a broad range of wind speed, it would have rather a higher performance at the higher, stable speed and the higher location (e.g., oceanic wind environment). Since the on-shore wind turbines have been installed at many places until now, there are many problems that is the seasonal variation of wind speed, the space availability for the installation, low-frequency noise and public complaint. Therefore, in this regard, the new business regarding to the large-scale wind farm would be a future barrier. Nonetheless, the offshore energy business will be one of the best candidates for the future development of energy harvesting, which is surely able to make a full size of stable facilities without any distraction to the surroundings.

Recently, Europe has been leading the offshore wind power industry, and Canada, China, and the USA are also devoting their attention. Most offshore wind farms usually have been installed in a shallow water of the near-shore. However, many scientists are currently interested in making the world's largest wind turbine and farther away from the land. The deeper the water depth is, the higher the cost of the offshore structure will be. Therefore, many concepts has been suggested to make an optimized design for floating the base platform. The concepts basically include the concrete caisson, the monofile, the jacket, and the floating type Musial(2004), Butterfield(2007). For a deep water structure, the floating type foundation is more economical than other foundations. There have been many researches on the dynamic characteristics of floating structure in order to reduce an undesirable motion in deep water Jang(2006). Offshore structures are mainly divided into three categories - Barge Platform(BP), Tension Leg Platform(TLP) and Spar Buoy platform(SBP). Among them, the most effective one for deep water (i.e., over 60~900m depth from the sea surface Musial(2006)) would be the SBP. SBP is a floating caisson which has a hollow cylinder inside the structure (i.e., similar to a very large buoy), which has a hull, moorings, topsides and risers.

To observe the dynamic responses arising from the upstream wind and wave load, the SBP is simply considered as a rigid floating body with flexible elements such as mooring cables. The offshore platform experiences a variety of external loads, which include wind, wave and current load and sometimes tides and earthquake, etc. If the behavior of platform is irregularly induced by the external forces, the power performance of wind turbine would be reduced and unstable. Therefore, these external loads should be evaluated exactly to get the oceanic environmental condition which is basically used for the boundary condition of numerical calculation Shoten(2001).

In order to get a boundary condition of ocean environment, the study gets some data from the MET office in a nearshore in South Korea (e.g., Tong-Young). The acquired wind and wave profiles are properly analyzed to get an inflow condition of the

wind/wave load acting on the body. The hydrostatic and hydrodynamic loads are formulated by a combination of the Morison formula and the pressure integration method. Based on the water depth and the wave period/height, the linear airy wave theory and non-linear Stokes wave theory can be selectively applied. In order to understand the dynamic response of the floating body and the mooring cables, we changed the fairlead position and the angle of the mooring cables.

## 2. MODELING OF THE FLOATING OFFSHORE WIND TURBINE

The offshore wind turbine generally consists of the machinery structure (rotor and nacelle) and the support structure (tower, platform and mooring system). For the engineering point of view, the rotating blade is not included and the shape of body is simplified. Fig. 1 shows the description for modeling the floating offshore wind turbine. The model size of SBP platform with the tension mooring cables was originally designed by KITECH (Korea Institute of Industrial Technology) and optimized for a practical use. To predict the multibody dynamics of the floating body, we used the commercial software, MSC.ADAMS. We assume that the tower and platform are all rigid bodies, and the mooring cables are all flexible. Since the diameter of the mooring cables is far less than the length, it has to be considered to be flexible body. In addition, each component of the floating body is linked in a fixed joint, including the connections of the platform and the mooring cables, the mooring cables and the seabed. (e.g., see the lock symbols in the Fig. 1.

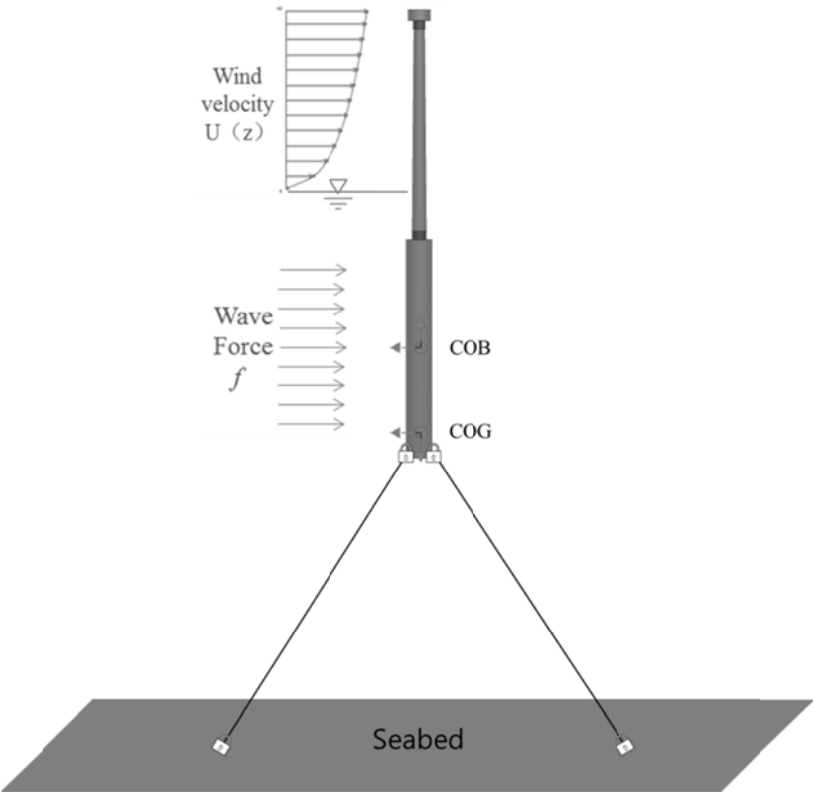


Fig. 1 The floating offshore wind turbine modeling

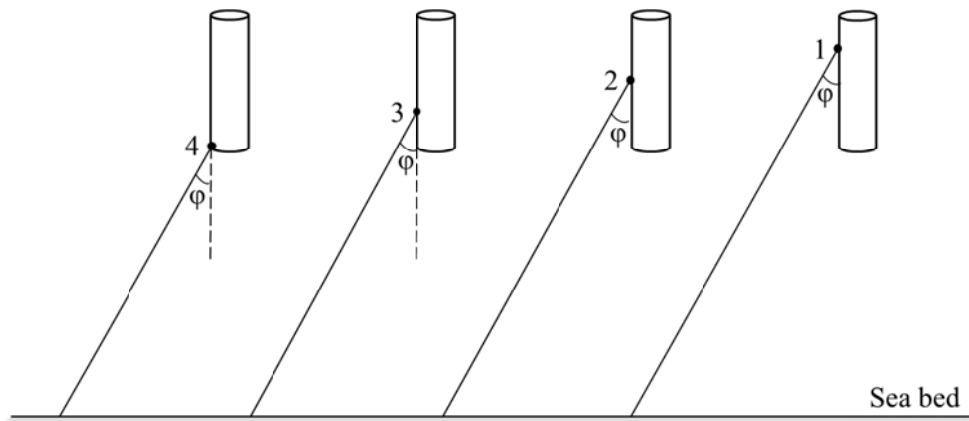


Fig. 2 The schematic diagram of the position and the connected angles

This study mainly focuses on the dynamical analysis when changing the characteristics of the mooring cables (i.e. angle and position, etc). Therefore, we set up a lot of models as shown in Fig. 2. Practically, the multiple mooring cables (i.e., three or four and beyond) connect axisymmetrically with multiple points on the floating body. Therefore, in this simplified figure, a body with a cable shows the connection angle and the position of fairleads. The effect of cable location was observed in four different positions as the fairlead between cables and platform, of which the positions 1 to 4 are located in the three-fourth, the mid-height, the one-fourth and the bottom of the platform (see Fig. 2) In addition, the effect of cable shape (i.e., the angle between the cable and the platform, which is defined as  $\varphi$ ) was also calculated in a same position, but in different angles  $\varphi$  of  $30^\circ$ ,  $45^\circ$  and  $60^\circ$ . For the details, all the specification of the floating offshore wind turbine was listed on the Table 1.

Table 1. The specification of the floating offshore wind turbine

Nacelle	Height	3.2 m	Platform	Height	65 m
	Mass	146,000 kg		Diameter	8 m
Tower	Height	65 m		Thickness of top	0.15 m
	Diameter of top	3 m		Thickness of bottom	0.23 m
	Diameter of bottom	4.5 m		Mass	2,648,000 kg
	Thickness of top	0.05 m		Mooring	Number of cable lines
	Thickness of bottom	0.1 m	Cable diameter		0.1 m
Mass	170,000 kg	Damping ratio	0.1		

In the software of MSC.ADAMS, there are three methods to set up the flexible bodies. Among them, we used the Flexible Beam connection enabling us to model the

cables of SBP platform properly, i.e., it builds the flexible bodies by discrete flexible link. Each cable was divided into 30 discrete parts, and each cable consists of 30 rigid elements and 29 flexible beams which will produce the deformation to prevent the floating body from being swept away when the environment loads apply to the floating body. The damping ratio of the flexible cable was set as 0.1, because in case that the value is not big enough, the cable will break down during the movement with the platform.

### 3. MODELING OF THE ENVIRONMENTAL LOADS

The following section defines the loads from external environment conditions in conjunction with the dynamical behavior of the floating offshore wind turbine. According to the DNV certificate DNV(2010), we obtain the guidance for calculating the environment loads acting on the structures. In the ocean environment, the atmospheric conditions include wind conditions and marine conditions (i.e. waves, currents, tides, ice, earthquake, erosion, soil properties, etc). For the simple approach, the most important wind and wave conditions are applied in the boundary condition and listed in the following parts.

#### 3.1 Wind load modeling

The wind speed distribution is significant for the offshore wind turbine design, as it determines the calculation of wind load. As we know, the wind speed varies with the time and the height above the sea surface. Therefore we should specify the wind speed for averaging time and the reference height. In the typical wind engineering application, the most commonly applied wind profile models are the power and the logarithmic law. Among them, we simply applied the power law profile as follows,

$$U_{(z)} = U_{(H)} \cdot \left(\frac{z}{H}\right)^\alpha \quad (1)$$

where  $U_{(z)}$  is the wind speed at the height ( $z$ ) from the sea surface;  $U_{(H)}$  is the reference wind speed at the reference height ( $H$ ) from the sea surface;  $\alpha$  is the exponent which depends on the terrain roughness. Note that in this study, the exponent  $\alpha$  is valued as 0.14. In addition, according to the statistical data suggested by KHOA (Korea Hydrographic and Oceanographic Administration), we defined the reference standard height ( $H$ ) as 5m above the sea surface, with the reference wind speed  $U_{(H)}$  as 5.43m/s. The wind load which induces the structure is generally calculated by the wind speed profile, and can be defined as Eq. (2). Regarding to the points on which the resultant force acts, the central node of each discrete part was chosen so that we modified the Eq. (2) by integrating it from the sea surface (0m) to the top height ( $h$ ) of the tower, which is listed in Eq. (3).

$$F_{(z)} = \frac{1}{2} \cdot C_D \cdot \rho_a \cdot A \cdot U_{(z)}^2 \quad (2)$$

$$F = \int_0^h \frac{1}{2} \cdot C_D \cdot \rho_a \cdot D \cdot \left[ U_{(H)} \cdot \left(\frac{z}{H}\right)^\alpha \right]^2 \cdot d_z \quad (3)$$

where the value of  $U_{(z)}$  in Eq. (3) has been replaced by Eq. (1);  $C_D$  is the drag coefficient associated with the body shape;  $\rho_a$  is the air density ( $1.225\text{kg/m}^3$ );  $A$  is the cross-sectional area normal to the direction of the wind force.

### 3.2 Wave load modeling

In the real situation, the ocean waves are irregular and random in the process of propagation. However, due to the lack of the real marine data as well as for simplifying the calculation, we focus on researching the regular waves. Nowadays, there are a lot of wave theories to describe the regular waves, such as the linear Airy theory, the non-linear Stokes second or higher order theories, the Cnoidal wave theory, the Solitary wave theory and so on. Regarding to these theories, there are three wave parameters to determine which wave theory is appropriate in a given problem. The wave parameters include the wave height  $H$ , the wave period  $T$  and the water depth  $d$ . Based on three wave parameters, the non-dimensional parameter  $S$  (see Eq. 4) and  $\mu$  (see Eq. 5) can be defined for determining the range of validity and the appropriate wave theory, for the details, see Chakrabarti(1987).

$$S = 2\pi \frac{H}{gT^2} \quad (4)$$

$$\mu = 2\pi \frac{d}{gT^2} \quad (5)$$

where  $S$  and  $\mu$  are the wave steepness and the shallow water parameter. Once the wave theory is selected, we can obtain the water particle velocity ( $u$ ) and the water particle acceleration ( $\dot{u}$ ), which are defined as:

$$u = \frac{\pi H}{T} e^{kz} \cos(kx - wt) \quad (6)$$

$$\dot{u} = \frac{2\pi^2 H}{T^2} e^{kz} \sin(kx - wt) \quad (7)$$

where  $z$  is the distance under sea surface;  $k$  is the wave number;  $x$  is the distance of propagation;  $w = 2\pi/T$  is the angle wave frequency;  $t$  is the time.

For designing the slender structural members, wave loads can be calculated using Morison's equation, which includes an inertia force proportional to acceleration and a drag force proportional to the square of velocity. The Morison's equation is a semi-empirical equation, and the force per unit length acting on the rigid platform is defined as Eq. (8):

$$f = f_{dx} + f_{ix} = \frac{1}{2} C_d \rho D u |u| + C_m \rho \frac{\pi D^2}{4} \dot{u} \quad (8)$$

where  $f_{dx}$  is the drag force;  $f_{ix}$  is the inertia force;  $\rho$  is the density of sea water ( $1023\text{kg/m}^3$ );  $D$  is the platform cylinder diameter;  $C_d$  and  $C_m$  are the drag coefficient and inertia coefficient separately.

Similar to get the wind load, we modified Eq. (8) by integrating it from the bottom ( $h_1$ ) of the platform to the top ( $h_2$ ) of the platform. Then we can apply this force at the center of the platform by the user functions. The modified equation is as follows:

$$F = \int_{h_1}^{h_2} f = \int_{h_1}^{h_2} \left( \frac{1}{2} C_d \rho D u |u| + C_m \rho \frac{\pi D^2}{4} \dot{u} \right) dz \quad (9)$$

Moreover, from the statistical data suggested by KHOA, we defined the wave height as 0.6m, the wave period as 2.8s and the water depth as 200m. Given that the modeling of the floating offshore wind turbine and the environment loads are provided, the numerical simulations are made and analyzed.

## 4. THE RESULTS AND DISCUSSIONS

### 4.1 The dynamic response analysis of the SBP platform with mooring cables

Firstly, the numerical simulations were carried out in the time domain. According to the results, we tried to analyze the non-linear dynamical characteristics under the coupling conditions, and furthermore to study the flexible effects of the mooring systems.

In Fig. 2, one of representative cases was the position 4 with the angle 30°, which is the case of the wind force mainly acting on the center of the tower (i.e., 353.43N), while the wave force mainly acting on the center of the platform. As shown in Fig. 3, the wave force is relatively complicating, which varies with time. Note that the wind and wave force direction is the same. By comparison, the wave force seems to be rather bigger than the wind force, which may reach about 200 times bigger. This phenomenon states that the wave environment has a greater influence on the offshore structures than the wind environment.

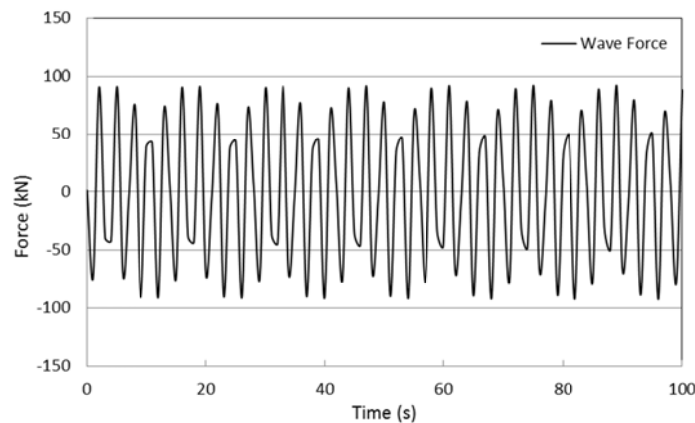


Fig. 3 The wave force acting on the platform

When the SBP platform moves under the wind and wave force, the cables also move with the platform. In other words, the motion of platform has an effect on the cables, and simultaneously, the cables have a restoring force to respond on the platform. This is called the coupling effects between the platform and the mooring system. Since we applied the wind and wave force at the same direction, so the SBP platform moves mainly on this direction, as shown in Fig. 4. The platform's movement appears to be periodic, and the amplitude of variation is not big (between -0.03m to

0.03m), which means that the platform remains relatively stable-state under the current wind and wave conditions.

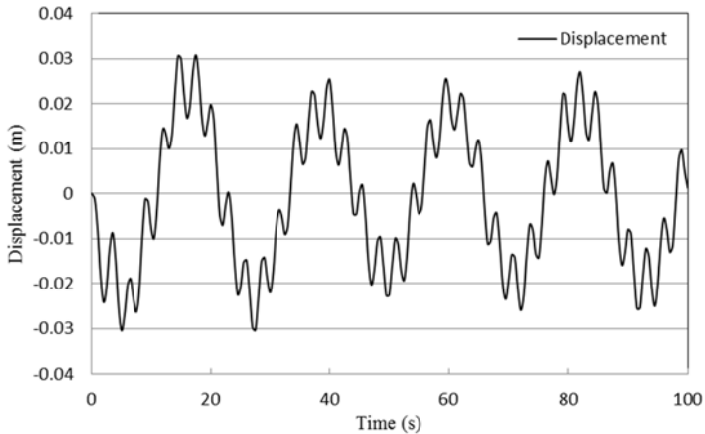


Fig. 4 The displacement of SBP platform at the mass center

To stabilize the SBP platform, the mooring system plays a significant role, which will produce a restoring force for the platform. We focused on the tensional variation of the mooring cables, as presented in Fig. 5. Firstly, as shown in Fig. 5 (a), we obtained the transient data of cable tension in 100 seconds. In the initial stage the tension seems to have a big change having some peak values, next the tension tends to stable state about 10 seconds. Secondly, we calculated again to obtain the tension data within a relatively long time of 3,600 seconds. The tension against time is plotted in Fig. 5 (b). Note that in Fig. 5 (b), we consider the primary tension data after neglecting the initial stage. As a whole, the tension force is between  $1.76 \times 10^6\text{N}$  to  $1.9 \times 10^6\text{N}$  which can keep the movement of the floating offshore wind turbine.

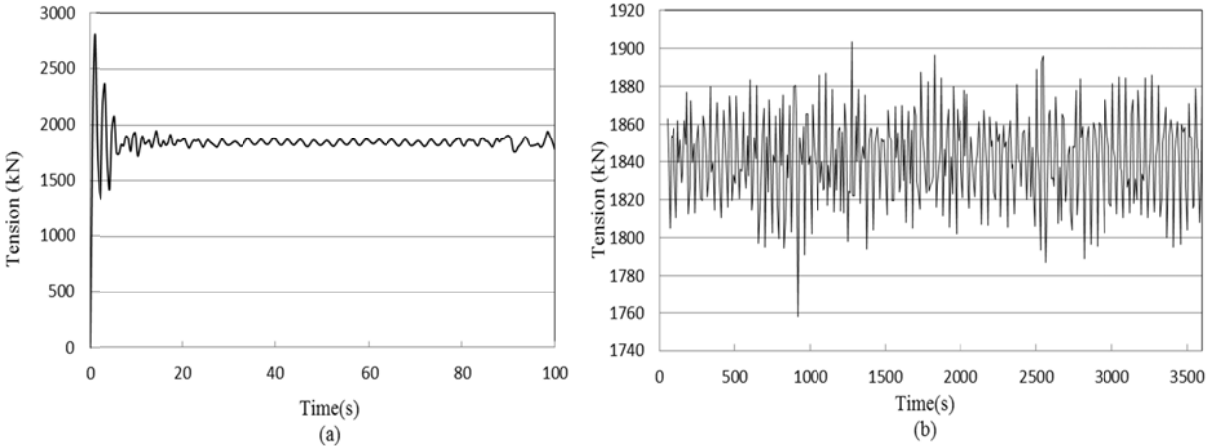


Fig. 5 The variation of tension force acting on the mooring cables

4.2 The effects of the fairlead position and the angle of mooring cables



Based on the case of position 4 with the angle  $30^\circ$ , we calculated more cases by changing the fairlead position and the angle of mooring cables. In Fig. 6, we compared the tension of the cables depending on the different fairlead positions. Note that when we changed the fairlead positions from position 1 to 4 (see Fig. 2), we should keep the same angle of mooring cables at each fairlead position. For example, in Fig. 6 (a), we compared the tension data from position 1 to 4 against the same angle of mooring cables  $30^\circ$ . In addition, Fig. 6 (b) presents the tension variation of the fairlead at different position, but at the same angle of  $45^\circ$ ; while Fig. 6 (c), presents the results at the same angle of  $60^\circ$ . Note that, the results were obtained within 100 seconds and neglected the data at the initial stage of about 40 seconds. When the angle of mooring cables is same, the change of fairlead positions seems to make little influence on the tension.

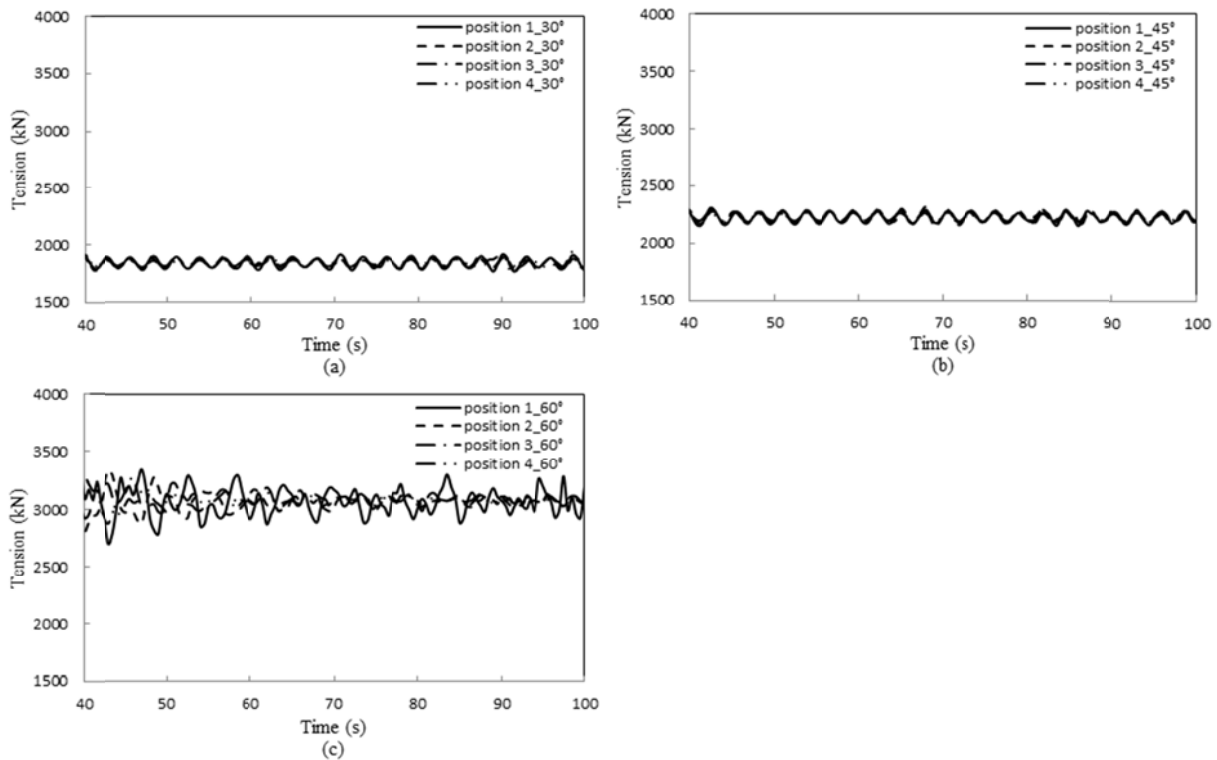


Fig. 6 The tension in the mooring cables with different fairlead positions

The immediate implication of Fig. 6 is that when the angle of mooring cables is  $30^\circ$  or  $45^\circ$ , the results agree well each other, but show a significant fluctuation when the angle changes to  $60^\circ$ . Therefore, we may conjecture that the angle of mooring cables has a higher influence on the tension than the fairleads position. For this reason, we calculated more cases about different angle of cables at the same fairlead position. Fig. 7 (a) represents the results of different angle at the same position 1, and the Figs. 7 (b), (c), (d) are the same arrangement but different position. The comparison shows that the bigger the angle becomes, the higher the tension force is. Furthermore, when the angle is  $30^\circ$ , the tension force is about  $1.8 \times 10^6$  N. When increasing the angle of  $15^\circ$  to  $45^\circ$ ,

the tension force increases about  $0.4 \times 10^6$  N, finally reaches to about  $2.2 \times 10^6$  N. However, as increasing the angle  $15^\circ$  to  $60^\circ$ , the tension force becomes about  $3.0 \times 10^6$  N, which increases about  $0.8 \times 10^6$  N (twice as much as  $0.4 \times 10^6$  N). The results show that the tension force seems not proportional to the angle of mooring cables.

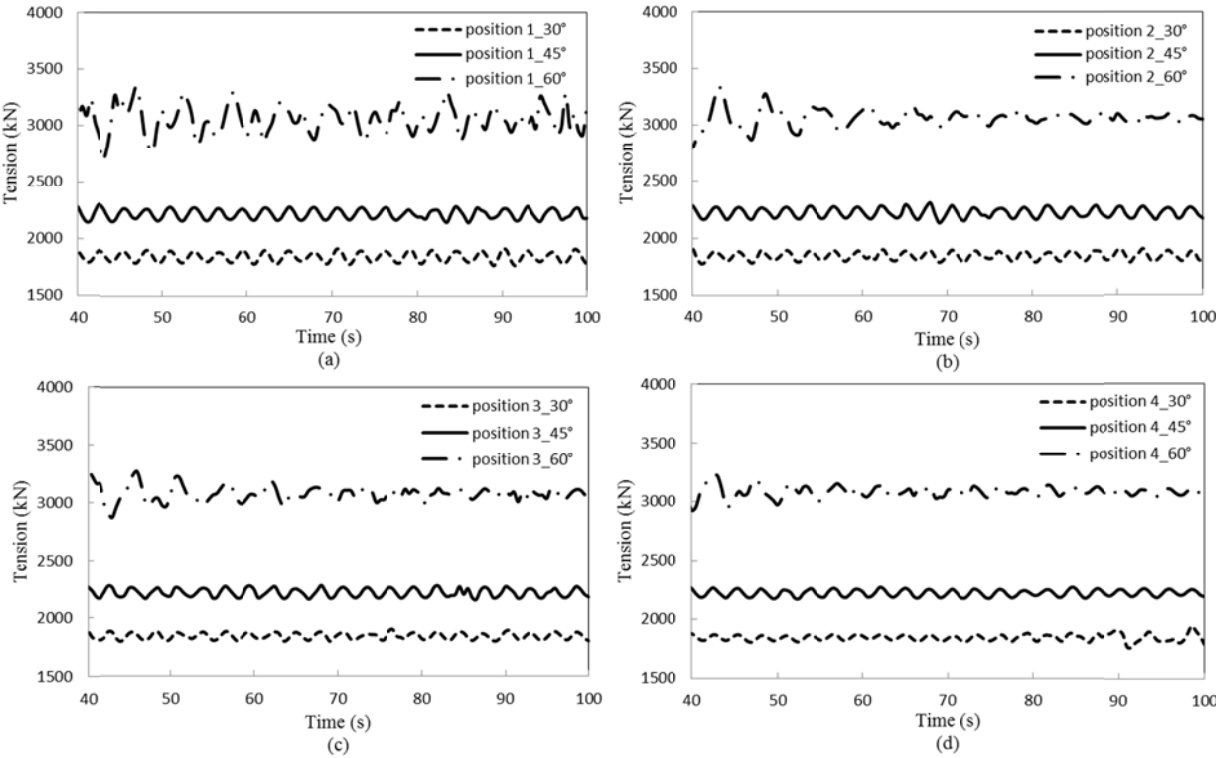


Fig. 7 The variation of tension force acting on the mooring cables with a variety of angle

**CONCLUSION**

Although more simulations and comparisons are needed to end up with the conclusions, the study has contributed in making the following conclusions:

- (1) The designed SBP platform with the tension mooring cables in this study can keep the movement under the designed wind and wave loads suggested by KHOA.
- (2) It is sure to have an interaction between the platform and the mooring system. The movements of the platform induces the motion of the mooring cables, while the mooring cables restrain the movements of the platform by a restoring force.
- (3) The angle between the platform and the mooring cables seems to have a higher influence on the tension of the mooring cables, while the fairlead position shows relatively less influence on the tension.

**ACKNOWLEDGEMENTS**

This work was supported by the Human Resources Development of the Korea Institute of Energy Technology Evaluation and Planning(KETEP) grant funded by the Korea

government Ministry of Knowledge Economy.(No. 20114030200070) and this research was also supported by the National Research Foundation of Korea (NRF) through the Human Resource Training Project for Regional Innovation

## REFERENCES

Butterfield, S., Musial, W., Jonkman, J. and Scalavounos, P. (2007), "Engineering Challenges for Floating offshore Wind Turbines," *NREL Conference paper*, USA, Cp-500-38776R.

Chakrabarti, S.K. (1987), *Hydrodynamics of Offshore Structures*, WIT Press.

DNV, (2010), *Environmental conditions and environmental loads*, DNV-RP-C205.

Ezio, S. and Claudio, C. (1998), "Exploitation of wind as an energy source to meet the world's electricity demand," *Journal of Wind Engineering and Industrial Aerodynamics*, **74**, 375-387.

Jang, J.S. and Sohn, J.H. (2011), "Analysis of Dynamic Behavior Of Floating Offshore Wind turbine System," *KSME-A.*, Vol. **35**(1), 77-83

Joselin, H.G.M., Iniyar, S., Sreevalsan, E. and Rajapandian, S. (2007), "A review of wind energy technologies," *Renewable and Sustainable Energy Reviews*, **11**, 1117-1145.

Musial, W. and Butterfield, S. (2006), "Energy from Offshore Wind," *NREL Conference paper*, USA, Cp-500-39450.

MSC/ADAMS. (2008), *User's Guide*, MSC, MI, USA.

Musial, W.D., Butterfield, S. and Boone, A. (2004), "Feasibility of Floating Platform Systems for Wind Turbines," *23rd ASME Wind Energy Symposium Proceedings*, Reno, Nevada, January, NREL/CP-500-34874.

Shoten, S. (2001), *Mega-Float Offshore Structure*, Dae Sun Publishers, Korea.

Wells, J. (2007), "Uncertainty about Future Oil Supply Makes It Important to Develop a Strategy for Addressing a Peak and Decline in Oil Production," *US GAO Peak Oil Report*, GAO-07-283. 1-82.